AIAA 92-0581

Product Formation in Chemically-Reacting Turbulent Jets

R. J. Gilbrech and P. E. Dimotakis

California Institute of Technology

Pasadena, CA

30th Aerospace Sciences Meeting & Exhibit

January 6-9, 1992 / Reno, NV

Product Formation in Chemically-Reacting Turbulent Jets*

Richard J. Gilbrech** and Paul E. Dimotakis†

Graduate Aeronautical Laboratories
California Institute of Technology
Pasadena, California 91125

Abstract

Results from experiments performed in a newly-constructed High Pressure Combustion Facility are presented. The experiments described here are designed to address Reynolds number effects on turbulent mixing and entrainment, and flame length in an axisymmetric, gas-phase turbulent reacting jet, in particular, over a large range of Reynolds numbers.

Introduction

Flame length in kinetically fast chemical reactions can be used as an important measure of Reynolds number effects and can be related to the rate of molecular mixing in turbulent jets (*e.g.*, Broadwell 1982). The experiments reported here rely on a new technique for measuring flame length, developed for the purpose of investigating Reynolds number, as well as other effects on flame length.

The facility is shown schematically in Fig. 1. The main apparatus is a 107 cm internal diameter by 183 cm length (1.64 m^3) pressure vessel, capable of operating at pressures from 0.1 atm to 15 atm. This allows an independent control of Reynolds number over 2.2 decades through the pressure, while holding other conditions constant (*e.g.*, flow-time scales, nozzle exit conditions, and buoyancy effects). Buoyancy effects, which scale as $\overline{\Delta\rho}/\rho_\infty$, where $\overline{\Delta\rho}$ is the average change in density, in the jet cone, owing to heat release and ρ_∞ is the ambient density, remain constant as the pressure is varied since both $\overline{\Delta\rho}$ and ρ_∞ scale directly with pressure.

** Currently with NASA, Stennis Space Center, MS 39529. AIAA Member.

† Professor, Aeronautics and Applied Physics. AIAA Associate Fellow.

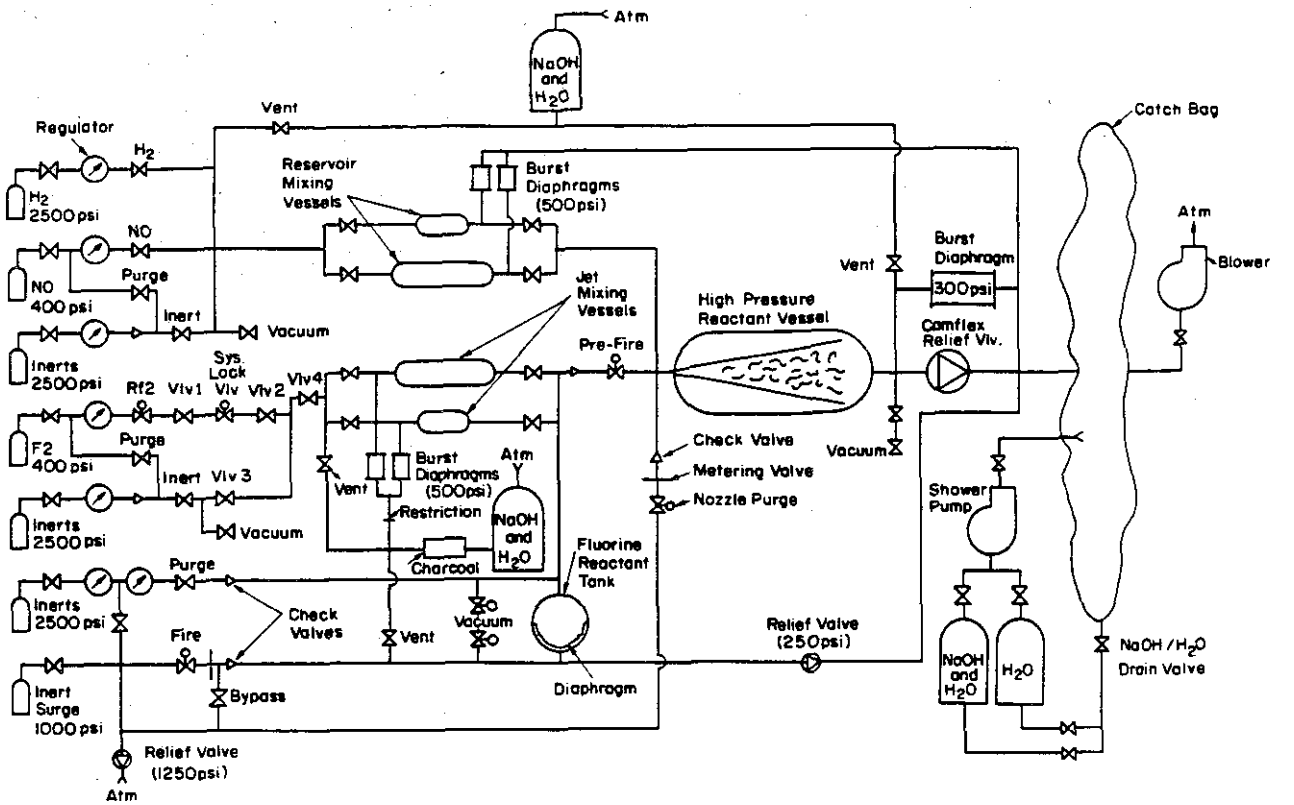

FIGURE 1 Schematic of the High Pressure Combustion Facility.

The chemical reactants chosen were F_2 and NO, diluted in N_2, for several reasons. First, these reactants are hypergolic, obviating the need for ignition sources and avoiding flame stability issues. The resulting chemical kinetics are very fast, ensuring that the rate of chemical product formation is limited by the turbulent mixing process and not by the chemical kinetics (high Damköhler number regime), even at the low reactant concentrations employed here. Finally, an additional attractive characteristic of this chemical system is the ability to produce a very low adiabatic flame temperature rise, $\Delta T_f \sim 7\,\mathrm{K}$ for the experiments described here, mitigating buoyancy effects while retaining an overall reaction rate in the turbulent jet that is kinetically fast. On the other hand, the choice of these reactants, *vis-à-vis* safety considerations, dictates a strict adherence to materials properties, as well as facility assembly and maintenance, and experiment operating procedures.

In these experiments, the jet issues from the bottom of the pressure vessel upwards, through a 2.5 mm internal exit diameter nozzle that protrudes into the vessel. The radial profile of the internal nozzle contraction section is designed as a 6^{th} order polynomial, optimized to avoid Taylor-Görtler vortices in the concave parts and for minimum exit boundary layer thickness. The outer nozzle profile is a paraboloid of revolution in an attempt to cater to the external potential flow field that is induced by the downstream entrainment.

The jet fluid is F_2, diluted in N_2. The reservoir fluid is NO, also diluted in N_2. Partial pressure techniques utilizing intermediate mixing vessels are used to accurately produce the desired jet and reservoir concentrations. The jet charge is contained in a smaller volume ($0.043\,m^3$) reactant tank which contains a teflon expulsion diaphragm. A metered sonic N_2 stream is fed to one side of the diaphragm, resulting in a fixed mass flow rate of jet gas through the nozzle. The reservoir pressure is held constant during the run with a Camflex pressure relief valve. See Fig. 1.

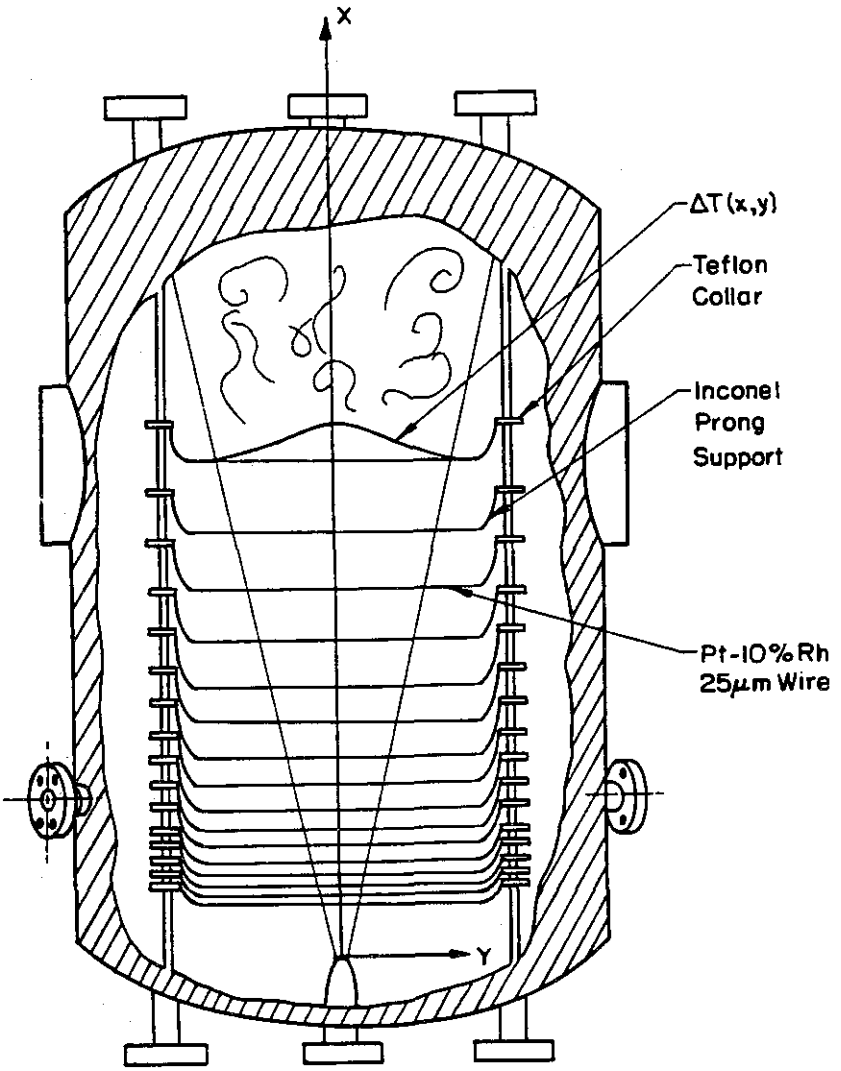

FIGURE 2 Schematic of jet geometry and diagnostics with the coordinate axes indicated.

The diagnostics utilized in these experiments were designed to give an accurate measure of flame length using constant current resistance thermometers. The thermometers are long (58 cm length), thin (25 μm diameter), Pt-10%Rh wires,

stretched across the jet centerline at 16 axial locations, from $x/d_0 = 30$ to 240. Here x is the streamwise (jet-axis) coordinate and d_0 is the nozzle internal exit diameter. The wires extend well beyond the edges of the turbulent jet cone, spanning the heat release and temperature rise regions, at all downstream locations. The wire streamwise locations were selected to give uniform spacing on a $\log_{10}(x/d_0)$ axis. This spacing was suggested in view of a conjecture by Dimotakis that the line-integrated measurements of temperature rise in the flame region would depend logarithmically on x/d_0. Figure 2 shows a schematic of the wires with the coordinate axes indicated.

Each wire formed one of the legs of a Wheatstone bridge circuit, whose output was amplified by a custom-built, low-noise signal amplifier, low-pass filtered by a third-order Butterworth filter with a knee set at 200 Hz, sampled at 500 Hz, and digitized to 12 bits. The wires were calibrated by allowing the interior of a slightly overpressurized vessel to equilibrate in temperature overnight and allowing the pressure to decrease over a few seconds in the morning. The resulting resistance change from each wire was recorded during the adiabatic cooling process. The small, common temperature drop experienced by each wire was estimated by measuring the internal vessel pressure using an electronic differential pressure transducer. In the course of a chemically reacting run, the mean temperature rise, determined from the change in total resistance of each wire, was estimated in this fashion to within, approximately, 30 to 50 mK.

The reason for choosing this particular measurement technique was motivated by the scaling laws of axisymmetric free turbulent jets. For the small heat release (temperature rise) employed in this experiment, the local wire resistance is a linear function of the local temperature. As a consequence, the total resistance of the cold wires, when stretched across the flame, yields an accurate estimate of the line-integrated heat release, *i.e.*, temperature rise, resulting from the chemical reaction.

At the end of the flame zone, shown schematically in Fig. 3, the F_2 has been completely consumed. No heat release occurs downstream of this location. Beyond the flame tip, at $x \simeq L_f$, the heat released by the reaction upstream is simply diluted by the subsequently entrained reservoir fluid. Therefore, for $x > L_f$, where L_f is the flame length, temperature excess is a conserved scalar.

Assuming that the flow achieves a self-similar temperature profile beyond the flame tip (as observed by Becker & Yamazaki 1978), the temperature rise for $x > L_f$ should obey the jet similarity law for a scalar quantity in a momentum-dominated jet. This similarity law can be derived from dimensional arguments (*e.g.*, Chen & Rodi 1980), has been verified experimentally (*e.g.*, Dowling & Dimotakis 1990), and is given by

$$\frac{\Delta T(x,y)}{\Delta T_f} = \kappa \frac{d^*}{x - x_0} g(\eta) , \qquad (1a)$$

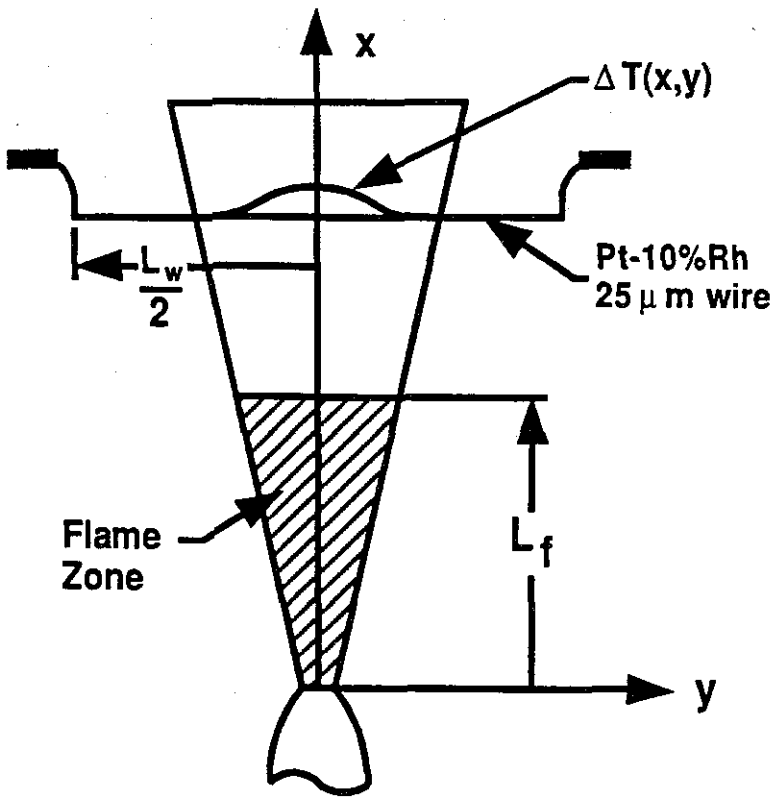

FIGURE 3 Schematic of the jet flame zone.

where $\Delta T(x,y)$ is the temperature rise at (x,y), y is the transverse coordinate, ΔT_f is the adiabatic flame temperature rise, κ is a constant (determined by experiment), d^* is the momentum diameter of the jet, $g(\eta)$ is the similarity mean profile function (determined by experiment), η is the similarity variable defined as

$$\eta \equiv \frac{y}{x - x_0} , \tag{1b}$$

with x_0 the virtual origin. The function $g(\eta)$ has a maximum value of 1 at $\eta = 0$ and goes to zero outside the jet edges ($\eta > 0.25$). The momentum diameter d^* is considered to be the proper normalization for the downstream coordinate of the jet (*e.g.*, Thring & Newby 1953, Avery & Faeth 1974, and Dahm & Dimotakis 1987), and is defined as

$$d^* = \frac{2\dot{m}_0}{\sqrt{\pi \rho_\infty J_0}} , \tag{2}$$

where $\dot{m}_0$ and J_0 are the nozzle exit mass and momentum fluxes, and ρ_∞ is the reservoir gas density.

Taking the line integral of Eq. 1a along y, at constant x (along a wire), and realizing that $g(\eta)$ goes to zero before $y = \pm L_w/2$, yields

$$\begin{aligned}\frac{1}{L_w}\int_{-L_w/2}^{L_w/2}\frac{\Delta T(x,y)}{\Delta T_f}\,dy &= \kappa\frac{d^*/L_w}{x-x_0}\int_{-L_w/2}^{L_w/2} g(\eta)\,dy \\ &= \kappa\frac{d^*/L_w}{x-x_0}\int_{-\infty}^{\infty} g(\eta)\,dy \\ &= \kappa\left(\frac{d^*}{L_w}\right)\int_{-\infty}^{\infty} g(\eta)\,d\eta \\ &\neq \mathrm{fn}(x)\ , \end{aligned} \tag{3}$$

where L_w is the span (length) of the wire.

As noted above, the measurement performed by each wire is the line integral of the temperature excess at constant x. This is given by

$$\frac{1}{L_w}\int_{-L_w/2}^{L_w/2}\Delta T(x,y)\,dy\ . \tag{4}$$

This quantity is analogous to the product thickness used for the shear layer (*e.g.*, Dimotakis 1989). In particular, the product thickness $\delta_P(x)$, normalized by L_w, will be defined as

$$\frac{\delta_P(x)}{L_w} \equiv \frac{1}{L_w}\int_{-\infty}^{\infty}\frac{\Delta T(x,y)}{\Delta T_f}\,dy\ . \tag{5}$$

The product thickness $\delta_P(x)$ is equal to the width of a top-hat temperature profile of height ΔT_f that yields the same area as that found under the $\Delta T(x,y)$ temperature rise profile for that x location. Equations 3 and 5 are equivalent to Eq. 4 divided by ΔT_f.

The time-averaged, line-integrated mean temperature rise measured at each wire beyond the flame tip, *i.e.*, for $x > L_f$, is expected to asymptote to a constant value. Accordingly, the line integral will rise to that asymptotic value as dictated by the cumulative mixing and chemical product formation up to that location for values of $x < L_f$.

Results and Conclusions

Figure 4 shows a sample of the raw data from the 16 wires spanning $x/d_0 = 30$ to 240, along with two reference wires placed outside of the jet cone at $x/d_0 = 0$ and 240, and the scaled velocity trace. Starting from the bottom trace and working upwards, the lowest trace is the reference wire at $x/d_0 = 0$ (partially obscured by the x-axis of the figure), then the 16 measurements from $x/d_0 = 30$ to 240, the other reference wire at $x/d_0 = 240$, and, finally, the scaled velocity trace. The reference wire at $x/d_0 = 0$ measures the temperature of the ambient reservoir fluid and the reference wire trace at $x/d_0 = 240$ indicates the arrival of hot recirculated products at the last measuring station, thus determining the temporal extent of uncontaminated data. The scaled velocity trace indicates the time required to establish steady state flow.

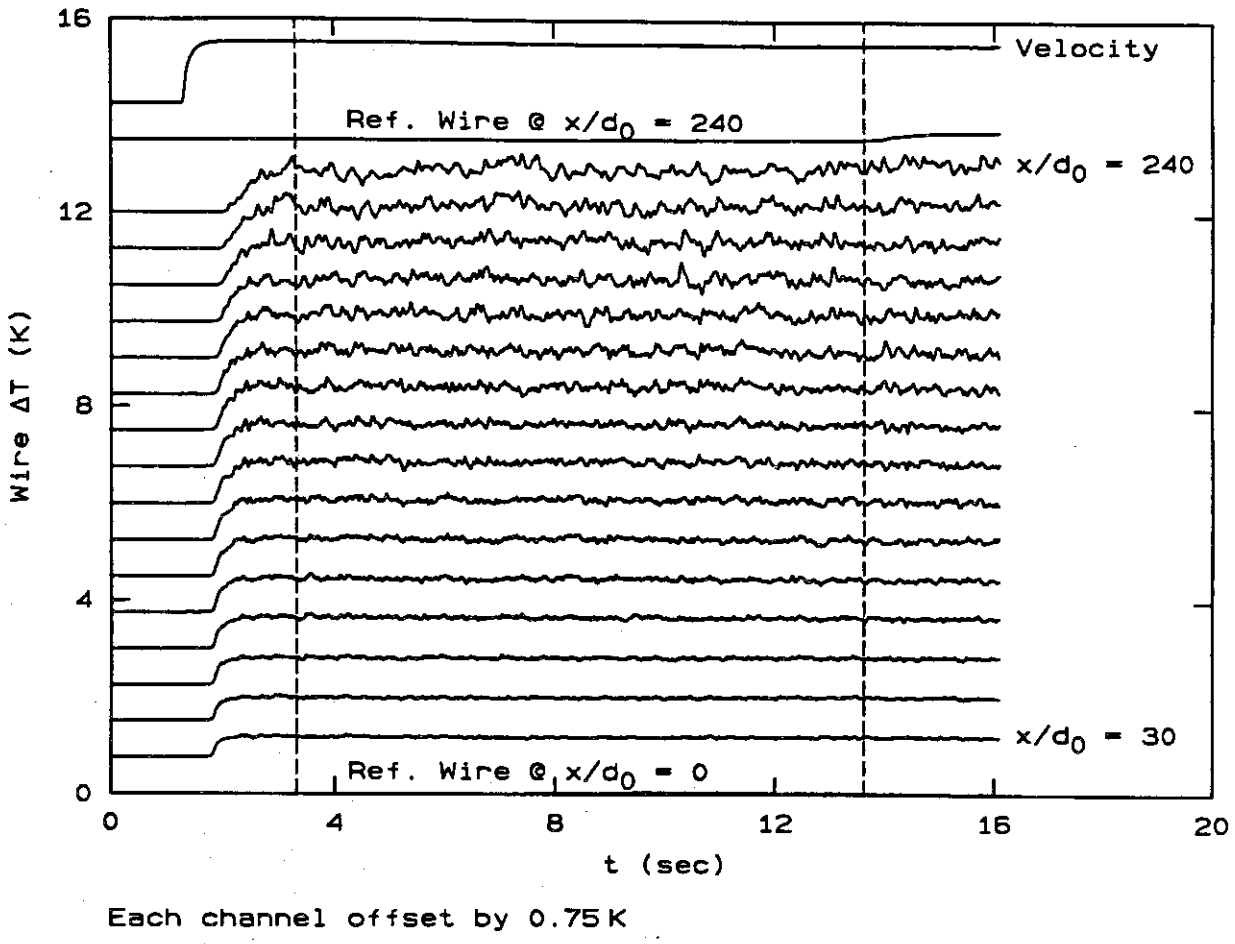

FIGURE 4 Sample traces of cold wire raw data for $\phi = 15$ and $\Delta T_f = 7$ K. Vertical dashed lines mark the averaging interval used for the corresponding data in Fig. 5. See text for details.

In the typical data in Fig. 4, note the small delay between the time the jet velocity has reached its steady value and the time the temperature rise is registered in the first wire at $x/d_0 = 30$. This time corresponds to the time required to flush the jet plenum of its original contents of reservoir fluid and charge it with the F_2-bearing jet fluid. Note also the increasing delay required for the reaction head to reach the wires at increasing x/d_0. The first vertical dashed line, at $t_1 \simeq 3.3\,\text{sec}$, marks the beginning of the time interval over which the data from each wire are to be averaged. The second vertical dashed line, at $t_2 \simeq 13.6\,\text{sec}$, marks the end of the averaging interval, prior to the arrival of the recirculating hot product gases, as registered on the top reference wire at $x/d_0 = 240$, outside the turbulent jet cone (second trace from the top). Note that the absolute span-averaged temperature change registered by the first wire is approximately 0.5 K. Small changes in the vessel temperature in the course of the run, as registered by the reference wire at $x/d_0 = 0$, are subtracted from the temperature registered by each wire and the difference for each wire is averaged over the selected (t_1, t_2) time interval for each run. As can be seen from the time-trace of the wire at $x/d_0 = 30$, the time-averaged mean temperature rise is determinable to a very good fractional accuracy.

The run recorded in Fig. 4 was for a stoichiometric mixture ratio of $\phi = 15$ and an adiabatic flame temperature rise of $\Delta T_f = 7\,\text{K}$. The stoichiometric mixture ratio ϕ represents the mass of reservoir fluid that must be entrained, mixed on a molecular scale, and reacted to completely consume a unit mass of jet fluid. It is defined by

$$\phi \equiv \frac{(Y_{F_2}/Y_{NO})}{(Y_{F_2}/Y_{NO})_{st}} \quad , \tag{6}$$

where, for a mixture of N species, the mass fraction, Y_i, is defined as

$$Y_i \equiv \frac{m_i}{\sum_{i=1}^{N} m_i} \quad , \tag{7}$$

with m_i equal to the mass of the i^{th} species in the mixture. The resulting averaged data points from the run in Fig. 4 are depicted in the corresponding $\phi = 15$ trace in Fig. 5.

Data for a number of stoichiometric mixture ratios ϕ and an adiabatic flame temperature rise of $\Delta T_f = 7\,\text{K}$ were processed, as described above, to produce the plot depicted in Fig. 5. The data correspond to the nondimensional product thickness (Eq. 5) and are plotted versus $\log_{10}(x/d^*)$ for the four stoichiometric mixture ratios ϕ indicated. The solid line for each set of data is a compound curve fit with a linear least squares fit to the ramp region and a cubic spline fit to the knee region, with the appropriate matching of value, slope, and curvature at the crossover. The flame length L_f will be defined as the 99% of maximum δ_P/L_w point, in the same spirit as the definition of a 99% boundary layer thickness. The expected

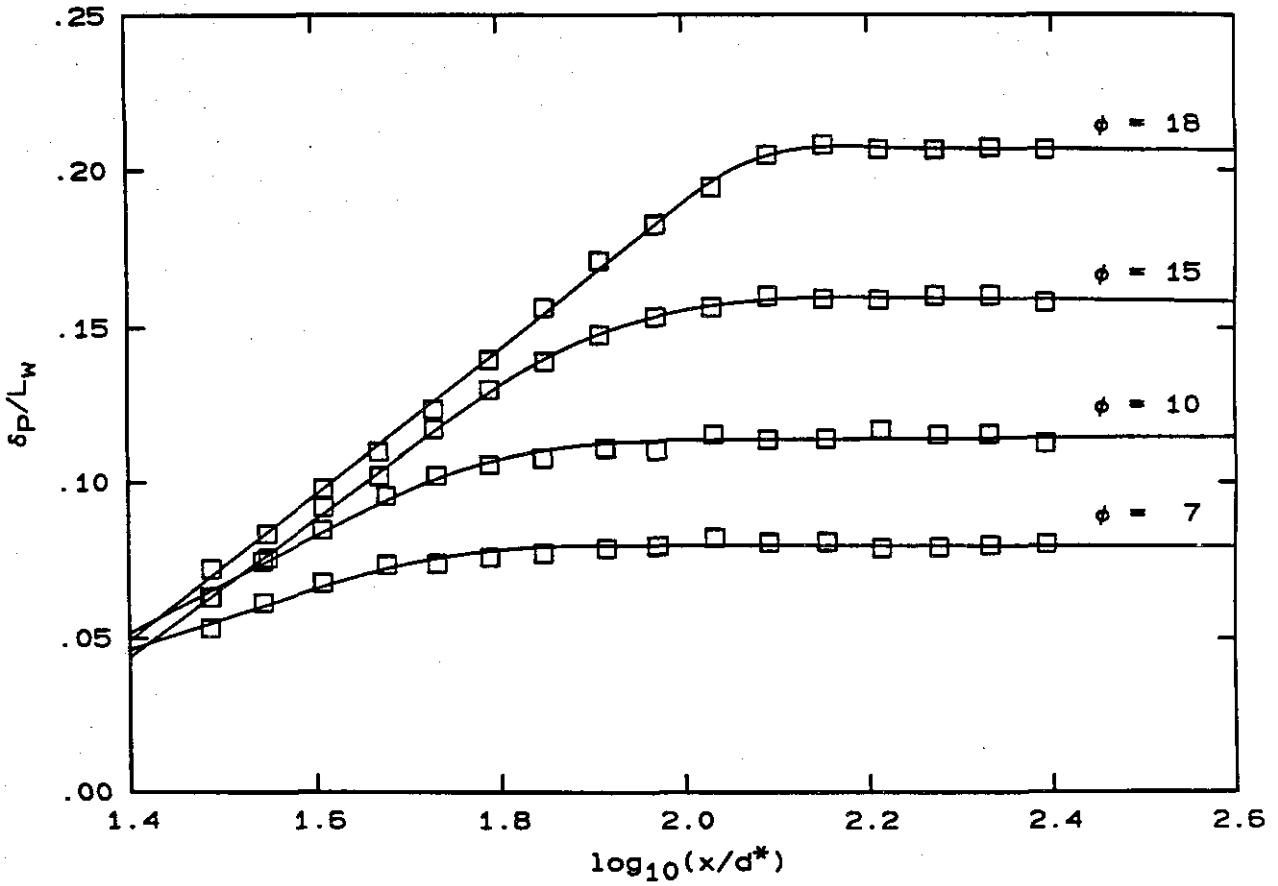

FIGURE 5 Sample plot of product thickness *vs.* $\log_{10}(x/d^*)$ for several ϕ's and an adiabatic flame temperature rise of $\Delta T_f = 7\,\mathrm{K}$.

increase in the integrated temperature rise is observed, as well as the asymptotic value at the end of the flame tip. The constant temperature level measured by the wires beyond the flame tip is proportional to ϕ, as can be shown from simple scaling arguments. The results display a linear behavior in the flame region, when plotted in the semi-logarithmic coordinates suggested by the choice of wire spacing, and corroborate the conjecture by Dimotakis mentioned above.

The results of additional experiments will be reported in the near future that address the flame length dependence on Reynolds number, the transition of the jet from a momentum-dominated to a buoyancy-dominated regime, and the effects of finite rate kinetics (Dahmköhler number) on mixing in the turbulent jet.

Acknowledgements

We would like to acknowledge the contributions of Godfrey Mungal who was responsible for the initial design of the High Pressure Reactant Vessel and Dan Lang for the data acquisition system and the the wire signal amplifier circuits, discussions and other assistance by Cliff Frieler, David Dowling, Jeff Hall, Paul Miller, Gene Broadwell and Ed Zukoski. Finally, we would like to acknowledge the invaluable contributions of Earl Dahl in the construction and operation of the facility and experiments.

This work was jointly funded by the Gas Research Institute through Contracts 5083–260–0878 and 5087–260–1467, and the Air Force Office of Scientific Research through Grants 83–0213 and 88–0155.

References

AVERY, J. F. AND FAETH, G. M. [1974] "Combustion of a Submerged Gaseous Oxidizer Jet in a Liquid Metal," *15th Annual Combustion Institute*, 501–512.

BROADWELL, J. E. [1982] "A Model of Turbulent Diffusion Flames and Nitric Oxide Generation. Part I," TRW Document No. 38515-6001-UT-00, EERC Final Report, PO No. 18889.

BECKER, H. A. AND YAMAZAKI, S. [1978] "Entrainment, Momentum and Temperature in Vertical Free Turbulent Difusion Flames," *Comb. and Flame* **33**, 123–149.

CHEN, C. J. AND RODI, W. [1980] *Vertical Turbulent Buoyant Jets. A Review of Experimental Data* (Pergammon Press, Oxford).

DAHM, W. J. A. AND DIMOTAKIS, P. E. [1987] "Measurements of Entrainment and Mixing in Turbulent Jets," *AIAA J.* **25**(9), 1216–1223.

DIMOTAKIS, P. E. [1989] "Turbulent Free Shear Layer Mixing," *AIAA* 27th *Aerospace Sciences Meeting*, 9–12 January 1989 (Reno, Nevada), AIAA–89–0262.

DOWLING, D. R. AND DIMOTAKIS, P. E. [1990] "Similarity of the concentration field of gas-phase turbulent jets," *J. Fluid Mech.* **218**, 109.

THRING, M. W. AND NEWBY, M. P. [1953] "Combustion length of enclosed turbulent jet flames," 4th *(International) Symposium on Combustion* (The Williams and Wilkins Co.), 97.